

Inhalation by Design: Novel Ultra-Long-Acting β_2 -Adrenoreceptor Agonists for Inhaled Once-Daily Treatment of Asthma and Chronic Obstructive Pulmonary Disease That Utilize a Sulfonamide Agonist Headgroup

Paul A. Glossop,^{*,†} Charlotte A. L. Lane,^{*,†} David A. Price,^{†,‡} Mark E. Bunnage,[†] Russell A. Lewthwaite,[†] Kim James,[†] Alan D. Brown,[†] Michael Yeadon,[‡] Christelle Perros-Huguet,^{‡,§} Michael A. Trevethick,[‡] Nicholas P. Clarke,^{‡,||} Robert Webster,[§] Rhys M. Jones,[§] Jane L. Burrows,[⊥] Neil Feeder,[⊥] Stefan C. J. Taylor,[⊥] and Fiona J. Spence^{||}

[†]Department of Worldwide Medicinal Chemistry, [‡]Allergy and Respiratory Research Unit, [§]Department of Pharmacokinetics, Dynamics, and Metabolism, ^{||}Department of Drug Safety, and [⊥]Department of Pharmaceutical Sciences, Pfizer Global Research and Development, Sandwich Laboratories, Ramsgate Road, Kent CT13 9NJ, U.K. [#] Present address: Pfizer Global Research and Development, Eastern Point Road, Groton, Connecticut 06340.

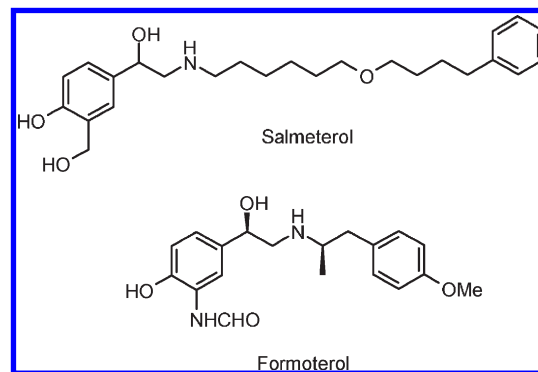
Received May 17, 2010

A novel series of potent and selective sulfonamide derived β_2 -adrenoreceptor agonists are described that exhibit potential as inhaled ultra-long-acting bronchodilators for the treatment of asthma and chronic obstructive pulmonary disease. Analogues from this series mediate very long-lasting smooth muscle relaxation in guinea pig tracheal strips. The sulfonamide agonist headgroup confers high levels of intrinsic crystallinity that could relate to the acidic sulfonamide motif supporting a zwitterionic form in the solid state. Optimization of pharmacokinetic properties was achieved through targeted introduction of a phenolic moiety to support rapid phase II clearance, thereby minimizing systemic exposure following inhalation and reducing systemically mediated adverse events. Compound **38** (PF-610355) is identified as a clinical candidate from this series, with in vivo duration of action studies confirming its potential for once-daily use in humans. Compound **38** is currently in advanced phase II clinical studies.

Introduction

Respiratory diseases such as asthma and chronic obstructive pulmonary disease (COPD^a) are highly prevalent diseases that affect millions of people worldwide. Long acting β_2 -adrenoreceptor agonists are a highly precedented drug class used for the treatment of asthma and COPD. There are currently two marketed long-acting β_2 -adrenoreceptor agonists (LABAs), salmeterol and formoterol (Chart 1), which exhibit sufficient duration of action to support twice-daily dosing regimens following inhaled delivery. However, neither of these agents are approved for once-daily dosing. A major area of current focus in the respiratory field is to identify novel, ultra-long-acting β_2 -adrenoreceptor agonists that are suitable for use as once-a-day inhaled agents, either as stand-alone therapies or for use in combination products with other bronchodilator and/or anti-inflammatory agents. The improved patient convenience and compliance associated with such once-a-day treatments, especially when delivered in convenient dry powder inhaler devices, is expected to support much more effective therapy for both asthma and COPD.

Chart 1



A number of reports from our laboratories and others have described various chemical series that offer promise as inhaled once-daily β_2 -adrenoreceptor agonists.^{1–9} Indacaterol (QAB-149) is the most advanced agent (Chart 2), having been recently approved as its maleate salt in the European Union (2009) and launched (2010) as the Onbrez Breezhaler for once-daily treatment of COPD.³ Advanced agents from other efforts include milveterol (GSK-159797),⁴ vilanterol (GSK-642444),⁵ and olodaterol (BI-1744-CL)⁶ that have largely been progressed to phase II trials in asthma and phase III trials in COPD (Chart 2). We have previously reported the design and profile of two novel series of β_2 -adrenoreceptor agonists exemplified by compounds **1**, **2**, and **3** (Chart 3).^{7–9} In addition, **1** and **3** have been disclosed as compounds that were selected as development candidates.¹⁰ Both compounds

^{*}To whom correspondence should be addressed. For P.A.G.: phone, +44 1304 649188; fax, +441304651821; e-mail, paul.glossop@pfizer.com. For C.A.L.L.: phone, +441304648231; fax, +441304651813; e-mail, charlotte.lane@pfizer.com.

^aAbbreviations: ACh, acetylcholine; cAMP, cyclic adenosine monophosphate; CHO, Chinese hamster ovary; COPD, chronic obstructive pulmonary disease; DDI, drug–drug interaction; DoA, duration of action; DPI, dry powder inhaler; DSC, differential scanning calorimetry; DVS, dynamic vapor sorption; EFS, electrical field stimulation; GPT, guinea pig trachea; LABA, long-acting β_2 -adrenoreceptor agonist; PXRD, powder X-ray diffraction; sGAW, specific airway conductance; TGA, thermogravimetric analysis.

Chart 2

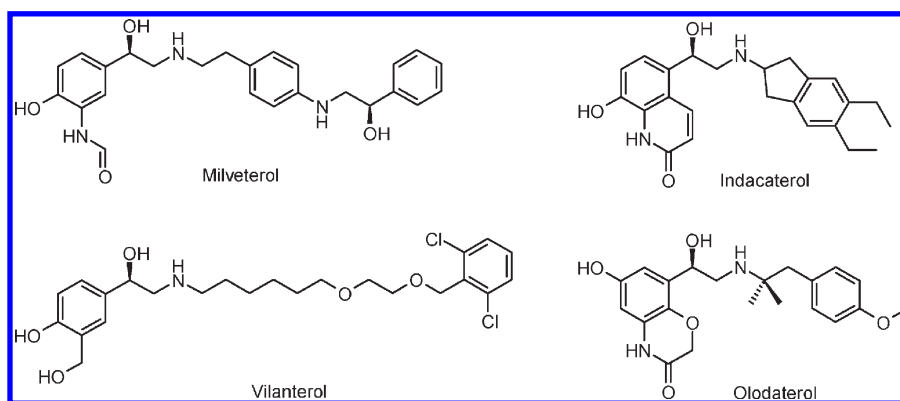
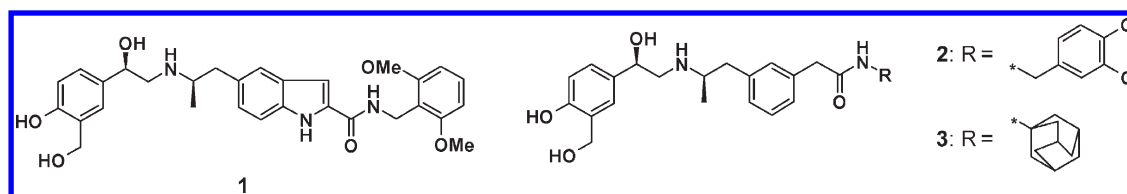
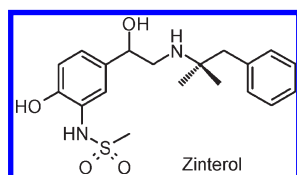
Chart 3. Structures of Previously Disclosed Pfizer β_2 -Adrenoreceptor Agonists

Chart 4



met our criteria for progression, including high levels of potency, long duration of action (DoA) in vitro and in vivo, and suitable pharmacokinetics for inhaled delivery (low oral absorption, rapid systemic clearance). However, while **3** possessed good material properties as its crystalline L-tartrate salt, compatible with delivery from a dry powder inhaler, it was generally found that securing suitable solid form characteristics in this conformationally flexible and lipophilic series presented a significant challenge. Therefore, as part of our strategy to identify additional development candidates, we sought to identify a differentiated series of β_2 -adrenoreceptor agonists with higher intrinsic crystallinity to simplify solid form identification and candidate selection.

In this paper we describe the discovery of a novel series of β_2 -adrenoreceptor agonists that combine the pharmacology profile required for once-daily dosing potential with the robust solid form attributes necessary to support convenient delivery in a preferred dry-powder inhaler device. This “inhalation by design” philosophy culminated in the discovery of compound **38** as a clinical candidate that is currently in advanced phase II studies for the treatment of asthma and COPD.

Chemistry

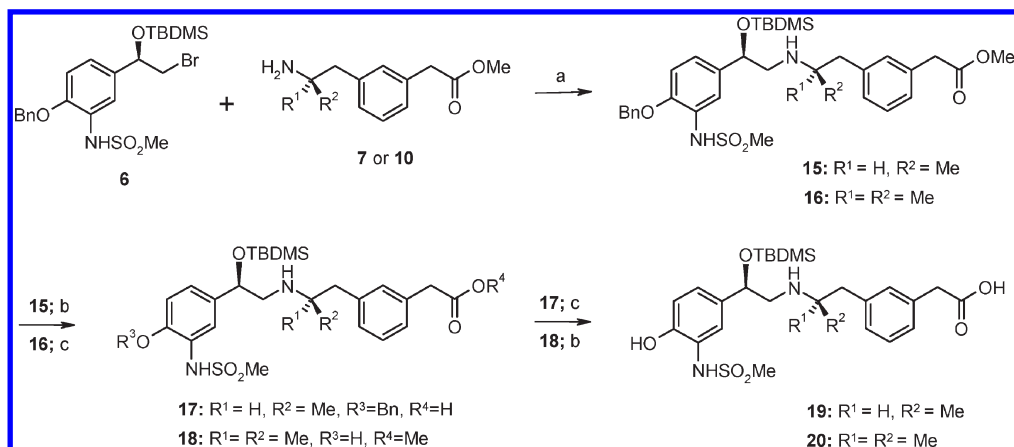
The target compounds in this paper have architecture similar to that of **2** (Chart 3) while utilizing the sulfonamide headgroup found in zinterol (Chart 4). The synthetic strategy for preparation of these targets was based upon two primary disconnections that lead to the key bromo alcohol “head”, amino ester “linker”, and amine “tail” fragments (Scheme 1).

The key sulfonamide headgroup **4** was prepared according to literature methods.¹¹ Selective N-mesylation to give **5** was followed by O-silylation to afford the protected intermediate **6** (Scheme 2).

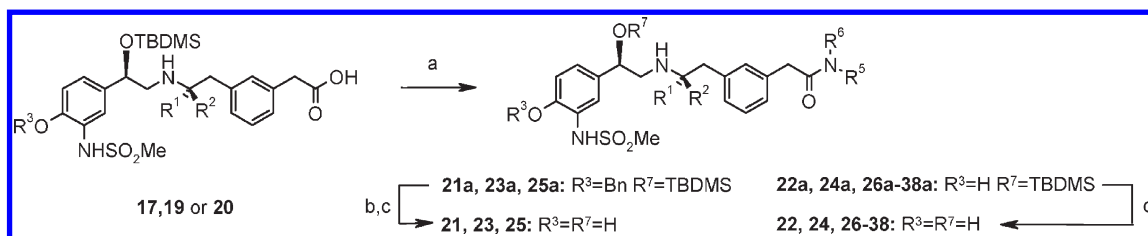
The monomethyl substituted linker **7** was prepared from 3-bromophenylacetic acid (Scheme 3). Esterification followed by palladium-mediated coupling with isoprenyl acetate gave the keto ester intermediate **8**. Reductive amination with *R*-(α)-methylbenzylamine gave the protected amino ester as a mixture of diastereomers in a 4:1 ratio (*R,R*-**9a**/*R,S*-**9b**). Selective crystallization of the desired *R,R* diastereomer **9a** as the hydrochloride salt was followed by transfer hydrogenation to give the aminoester **7** in good yield and high enantiomeric excess (Scheme 3).

The 1,1-dimethyl substituted linker **10** was prepared from 2,2'-(1,3-phenylene)diacetic acid (Scheme 4). Esterification of the diacid with ethanol gave the diester **11**, which was equilibrated with further diacid under acidic conditions to give a statistical mixture of the desired monoester **12**, together with diacid and diester. Treatment of the monoester **12** with excess methyl Grignard reagent in tetrahydrofuran gave the tertiary alcohol **13**. Standard Ritter conditions with acetonitrile were used to convert the alcohol to the acetamide; however, subsequent cleavage of the resulting acetamide proved problematic.¹² Treatment of the acetamide in refluxing sodium hydroxide in ethylene glycol resulted in decomposition, and acid hydrolysis was very slow. Further examination of the literature identified a modified Ritter procedure, using chloroacetonitrile rather than acetonitrile as the nitrogen source.¹³ Yields for the rearrangement reaction increased, and the resulting α -chloroacetamide **14** was readily cleaved by treatment with thiourea in refluxing acetic acid, followed by esterification to give the aminoester **10** in good yield (Scheme 4).

Coupling of **6** and the linkers **7** and **10** was effected by direct displacement of the bromide in the absence of solvent to give the key ester intermediates **15** and **16** (Scheme 5). The use of solvent and triethylamine as base was investigated; however, no advantage was found over the neat reaction. Ester hydrolysis of template **15** with aqueous lithium hydroxide gave the

Scheme 5^a

^a Reagents: (a) neat, 90 °C, 16–72 h, 58–80%; (b) LiOH, THF, 48–72 h, 90–100%; (c) 20% Pd(OH)₂/C, NH₄HCO₂, EtOH, 85 °C, 3 h, 65–84%.

Scheme 6^a

^a Reagents: (a) R⁶R⁵NH, 1-hydroxybenzotriazole, 1-(3-dimethylaminopropyl)-3-ethyl carbodiimide, ^tPr₂NEt, DMF, 18 h, 31–85%; (b) 20% Pd(OH)₂/C, NH₄HCO₂, EtOH, 85 °C, 3 h; (c) NH₄F, EtOH, H₂O, 50 °C, 18 h, 38–93%.

interest given their capacity for formation of hydrogen-bonding interactions and salt bridges and their presence in the headgroup of the β_2 -adrenoreceptor agonist zinterol (Chart 4).

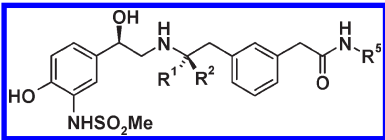
In addition to its potential to confer crystallinity, with the sulfonamide moiety being one of the most effective H-bond donors, it also had the potential to further reduce oral absorption across the gut wall in a manner consistent with our “inhalation by design” objectives, namely, to minimize systemic exposure and maximize therapeutic index (TI) through reduced oral bioavailability (of the swallowed fraction following inhalation) and increased hepatic clearance.⁸ There have been numerous analyses investigating molecular properties that influence good oral absorption/bioavailability, and a feature that most of them agree upon is the preference to minimize hydrogen bonding character.¹⁵ One example of this type of analysis is Lipinski’s so-called “rule-of-five” (Ro5), in which H-bond donors (<5) and H-bond acceptors (<10) represent two of the four rules suggestive of good oral absorption.¹⁶ Retaining the propensity for hydrogen bonding and molecular properties consistent with non-“Ro5” compliance was therefore an imperative part of our design strategy that sulfonamides also appeared to complement. Consequently, we decided to focus our immediate efforts on incorporating this headgroup into our novel series of phenethylamide containing β_2 -adrenoreceptor agonists.

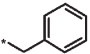
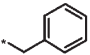
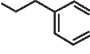
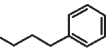
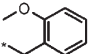
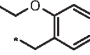
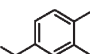
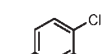
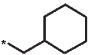
Initial amide analogues were prepared using the (*R*)-methylphenethylamine linker found in development candidate **3**, as a design strategy to retain desirable properties such as high levels of potency, long DoA, and suitable pharmacokinetics while introducing the sulfonamide headgroup to assess its impact on these properties and its potential for crystallinity. Project experience also taught us that relatively lipophilic compounds ($\log D \geq 2$) and molecular architecture similar to salmeterol

were important considerations as design criteria to obtain sufficient DoA to meet our objectives.^{7–9}

Excellent β_2 -adrenoreceptor potency, agonism (equivalent to isoprenaline), and selectivity were retained through incorporation of the sulfonamide motif, as illustrated by initial target **21**, confirming the need to fully explore this expression of our novel template (Table 1). However, despite the excellent potency of **21**, it was clear that incorporation of the sulfonamide group had led to significant reduction in lipophilicity ($\log D < 2$) that was inconsistent with our design strategy. Consequently, a range of sulfonamide analogues were synthesized to establish SAR, while incrementally increasing $\log D$. These data clearly demonstrated that a wide variety of amide substitution was tolerated, including CH₂ homologation (**23**, **24**), aromatic substitution (**25–28**), and cycloalkyl substitution (**29**). Importantly, these analogues also demonstrated that potency and selectivity were achievable with a range of lipophilicity that extended beyond our design criteria (**28**; $\log D = 2.4$) and as such had potential to deliver long DoA in vitro. Replacement of the (*R*)-methyl group adjacent to the basic nitrogen with the gem-dimethyl moiety (**21** vs **22**) retained the desired levels of both β_2 -adrenoreceptor potency and selectivity over the β_1 -adrenoreceptor.⁸ Given the preference of the β_2 -adrenoreceptor for molecules with an (*R,R*)-configuration (**1**, formoterol),^{7,17} these data further illustrate that the (*R*)-methyl substituent makes the key interaction regarding β_2 potency and selectivity (driven by this β_2 potency) while the (*S*)-methyl substituent makes neither significantly positive nor negative receptor–ligand interactions. Incorporation of gem-dimethyl substitution was also advantageous because it removed one of the two stereogenic centers from the molecules, thereby reducing synthetic complexity. Overall, it

Table 1. β_2 Potency, β_1 Selectivity, clogP, log *D*, and In Vitro Guinea Pig Trachea Data for Compounds **21**–**29**



	Compound	R ¹	R ²	R ⁵	β_2 EC ₅₀ ^a (nM)	β_1/β_2 ^b	clogP/ logD	Guinea pig trachea potency ^c	Guinea pig trachea duration of action ^d (h)
21		H	Me		0.027	16000	1.7 1.0	n.d. ^e	3.24 (n=2)
22		Me	Me		0.023	7500	2.1 -	-	-
23		H	Me		0.040	1800	1.8 -	-	-
24		H	Me		0.042	3400	2.2 1.7	n.d. ^e	5.85 (n=2)
25		H	Me		0.040	5600	1.6 1.2	n.d. ^e	4.22 (n=2)
26		H	Me		0.048	3300	2.2 1.6	n.d. ^e	6.20 (n=2)
27		H	Me		0.056	3700	2.6 2.0	n.d. ^e	6.74 (n=2)
28		Me	Me		0.066	1700	3.4 2.4	0.67	8.34 (n=4)
29		H	Me		0.032	3100	2.3 -	n.d. ^e	5.79 (n=5)
	2				0.024	5300	3.1 / 2.6	0.40	9.00 ^f (n=4)
	3				0.064	1300	2.4 / 2.1	0.69	6.35 (n=5)
	Zinterol				0.054	4900	1.5 / 0.6	0.76	3.40 (n=2)
	Salmeterol				0.070	7900	3.0 / 2.1	1.0	6.97 (n=5)

^a Potency and efficacy at human recombinant β_2 -adrenoceptors expressed in CHO cells assessed as elevations in cAMP. In this assay, all compounds appeared to be full agonists in comparison to isoprenaline control. ^b Ratio of EC₅₀ values generated at human recombinant β_1 - and β_2 -adrenoceptors expressed in CHO cells assessed as elevations in cAMP. Ratio is quoted to 2 significant figures. ^c EC₅₀ potency in the in vitro guinea pig trachea assay, quoted relative to salmeterol, such that a compound twice as potent will be quoted as 0.5. ^d Duration of action (DoA) was calculated as the time taken in hours for the EFS response to recover by 50% of the inhibition induced by an *E*_{max} concentration of the test compound. ^e n.d.: EC₅₀ and potency relative to salmeterol not determined to facilitate rapid assessment of duration of action at an estimated *E*_{max} concentration of test compound. ^f Incomplete (<100%) recovery after 14 h. Fully reversible by selective β_2 antagonist 2-butanol, (2*R*,3*R*)-rel-1-[2,3-(Dihydro-7-methyl-1*H*-inden-4-yl)oxy]-3-[(1-methylethyl)amino]-2-butanol.

was demonstrated that levels of β_2 -adrenoreceptor potency and selectivity comparable to those of previously developed series (**2**, **3**) were achievable in this sulfonamide template.^{8,9}

To assess the potential of these sulfonamide compounds to deliver long DoA, the effect of **21**, **24**–**29**, zinterol, and salmeterol on airway smooth muscle was investigated in vitro using guinea pig tracheal strips (Table 1). The pharmacology of β_2 agonists in this model is well documented and correlates well with clinical data, giving a measurement of potency, efficacy, and DoA.¹⁸ As anticipated, benzylamide **21** was found to have short in vitro DoA (3.24 h, log *D* = 1.0) when compared to salmeterol (6.9 h, log *D* = 2.1) and similar in vitro DoA when compared to zinterol (3.4 h, log *D* = 0.6), probably due to its significantly reduced lipophilicity. Consistent with our design hypothesis, tracheal data for compounds **24**–**29** revealed that increasing lipophilicity in this series resulted in the anticipated increase in DoA, for example, phenpropylamide **24** (5.85 h, log *D* = 1.7) vs benzylamide **21**,

and ethoxybenzylamide **26** (6.2 h, log *D* = 1.6) vs methoxybenzylamide **25** (4.22 h, log *D* = 1.2). Moreover, dimethylbenzylamide **27** (6.74 h, log *D* = 2.0) possessed similar DoA and measured log *D* to both salmeterol and development candidate **3**, while the yet more lipophilic 3,4-dichloro analogue **28** (8.34 h, log *D* = 2.4) demonstrated superior DoA to salmeterol. In addition, **28** was essentially equipotent with salmeterol, zinterol, and **3** in terms of their tracheal and cell based EC₅₀ data. Cyclohexylamide **29** also satisfied the general lipophilicity–DoA relationship. These in vitro data provided further evidence that this sulfonamide template could deliver the overall β_2 -adrenoreceptor agonist pharmacology that we required.

Following this demonstration of pharmacology, we turned to our attention to the key, overriding project objective: obtaining high levels of intrinsic crystallinity to simplify solid form identification and selection for inhaled dry-powder delivery. Consequently, a number of crystallization experiments

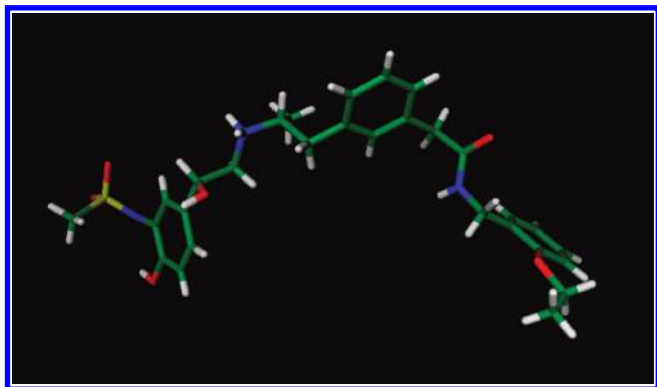


Figure 1. Small molecule X-ray crystal structure of compound **26**.

were performed with a selection of compounds from Table 1, using a variety of standard techniques and conditions. It soon became apparent that isolation of crystalline material in this series was readily achievable. In fact, crystallinity was such that it enabled generation of single crystal X-ray structures, as exemplified by compound **26** (Figure 1). The structural information gleaned from this X-ray not only confirmed the stereochemistry and solid state conformation but also revealed a potential driving force for crystallization: intramolecular protonation of the basic amine with the acidic sulfonamide proton. The formation of this internal salt, or zwitterion, may provide the crucial intermolecular salt bridge or hydrogen bonding interactions that order the crystal lattice and induce crystallinity.

The zwitterionic potential of **26** and these sulfonamide analogues in general is supported by **28**, whose pK_a values were measured as 8.93 and 7.97 for the amine and sulfonamide, respectively. Compound **28** was also found to be crystalline by powder X-ray diffraction (PXRD) with additional analysis by solid state Fourier transform infrared (FTIR) spectroscopy providing evidence for strong absorption bands at wavelengths characteristic of secondary ammonium ($R_2NH_2^+$) N–H stretching/bending vibrations. This crystalline form of **28** possessed a high melting point (195 °C) and was nonhygroscopic (<1.3% water uptake at 90% relative humidity), demonstrating that the key material properties for compatibility with a dry-powder inhaler device could be secured within this series.

As reported, compounds from previous saligenin series (**1**, **2**, and **3**) displayed suitable pharmacokinetics for inhaled delivery as a result of low oral absorption and rapid clearance from the systemic compartment, primarily through phase I cytochrome P450 (CYP) mediated metabolism.^{7–9} While we were confident that this would be the case for sulfonamide analogues **21–29**, we were keen to explore the possibility of introducing additional routes of metabolism to further maximize clearance, increase TI, and mitigate potential drug–drug interactions (DDI). Following a review of non-P450 mediated metabolic pathways, we identified glucuronidation as a clearance route of interest to us. Glucuronidation is a well documented high capacity phase II metabolic pathway that covalently conjugates glucuronic acid from UDPGA (uridine-5'-diphosphoglucuronic acid) to lipophilic substrates via UGT enzymes (uridine-5'-diphosphoglucuronosyl transferases).¹⁹ The glucuronide metabolites produced are polar, are water-soluble, and consequently undergo renal or biliary elimination. Glucuronidation is acknowledged as the major glycosylation reaction and is responsible for the detoxification of both

endogenous compounds and xenobiotics; consequently, it is a major source of drug inactivation and therefore appeared ideally suited to our objectives. Carboxylic acids and phenols are among the most commonly glucuronidated functional groups (although a variety of other moieties have precedent), but we were concerned that the addition of carboxylic acids to our template would negatively affect DoA as a result of introducing significant polarity and ionization. In addition, carboxylic acids give rise to potentially reactive acylglucuronide metabolites that we felt were an unnecessary drug safety risk to introduce, despite the anticipated low dose of these inhaled agents (≤ 1 mg). Consequently, we chose to incorporate phenols as the metabolic handle to assess glucuronidation while seeking to retain the desired crystallinity and β_2 -adrenoreceptor pharmacology of sulfonamide analogues **21–29**.

The β_2 -adrenoreceptor agonist pharmacophore is predicted to require an aromatic ring that makes hydrophobic interactions with Phe-290, associated meta- and para-H bond donors that form a hydrogen bonding network with Ser203, -204, and -207, and a key amino alcohol motif that makes hydrogen bonding and salt bridge interactions to Asn293 and Asp113, respectively.²⁰ As a result of these requirements, the vast majority of β_2 -adrenoreceptor agonist headgroups contain one or two phenols, as illustrated by the endogenous ligand norepinephrine (adrenaline) and examples such as salmeterol, formoterol, and zinterol. However, while there is some evidence that phenols such as that present in salmeterol are glucuronidated in rat, the extent of glucuronidation in humans is much less significant.²¹ Consequently, it appeared that incorporation of phenols for glucuronidation required more bespoke medicinal chemistry design than use of simple phenolic head groups. Given the critical β_2 -adrenoreceptor agonism, crystallinity, and synthetic complexity imparted by the sulfonamide headgroup, we decided to retain this fragment in its entirety, choosing to introduce phenolic substitution on the more synthetically accessible benzylamide tail portion. Phenolic analogues **30–38** were subsequently synthesized to assess the effect of different phenols on β_2 -adrenoreceptor potency, selectivity, DoA, crystallinity, and glucuronidation in this sulfonamide template (Table 2).

Phenolic substitution was generally well tolerated across a variety of amide expressions and compared well with previous sulfonamide SAR (Table 1). For example, excellent levels of β_2 -adrenoreceptor potency, agonism (equivalent to isoprenaline), and selectivity were observed for chlorophenol analogues **30**, **32**, and **34** and dimethylphenol **35**. These data illustrated that both ortho- and para-phenols (**32** vs **30**) were equally potent and selective. Dichlorophenol **33** and *N*-ethyl analogue **31** showed slightly reduced β_2 potency (~ 8 - to 18-fold) and consequently reduced selectivity over β_1 activity, when compared to analogues **32** and **30**, respectively. Similarly, sterically demanding phenols such as naphthol **36** and biaryl analogues **37** and **38** also displayed slightly reduced but good levels of β_2 potency (β_1 selectivity was also reduced for these analogues).²² Importantly, the β_2 potency and selectivity of phenolic sulfonamide analogues **30–38** were demonstrated over a range of lipophilicity that suggested the potential to deliver long DoA in vitro.

The effect of **30–38** on airway smooth muscle was investigated using the previously described in vitro guinea pig trachea assay. Pleasingly, the majority of these phenolic analogues displayed high levels of potency and long DoA (Table 2). The exceptions to this were **34** (3.66 h) and **35** (4.59 h), both of which had significantly shorter DoA. It is interesting to note that these

Table 2. β_2 Potency, β_1 Selectivity, clogP, log *D*, and In Vitro Guinea Pig Trachea Data for Compounds **30**–**38**

NHSO₂Me

	Compound R ⁵	R ⁶	β_2 EC ₅₀ ^a (nM)	β_1/β_2 ^b	clogP/ logD	Guinea pig trachea potency ^c	Guinea pig trachea duration of action ^d (h)
30		H	0.020	7300	2.4 1.2	n.d. ^e	6.80 (n=6)
31		Et	0.37	210	2.9 1.6	n.d. ^e	8.49 (n=3)
32		H	0.017	7000	2.4 1.6	0.10	6.00 (n=4)
33		H	0.13	560	2.9 2.0	1.0	8.02 (n=2)
34		H	0.091	1600	2.6 0.8	n.d. ^e	3.66 (n=2)
35		H	0.045	3700	2.3 1.1	n.d. ^e	4.59 (n=3)
36		H	0.21	730	2.6 1.3	0.10	6.17 (n=3)
37		H	0.24	1300	3.3 -	0.82	6.57 (n=3)
38		H	0.26	220	3.3 1.9	0.31	6.23 (n=6)
	28		0.066	1700	3.4 / 2.4	0.67	8.34 (n=4)
	3		0.064	1300	2.4 / 2.1	0.69	6.35 (n=5)
	Zinterol		0.054	4900	1.5 / 0.6	0.76	3.40 (n=2)
	Salmeterol		0.070	7900	3.0 / 2.1	1.0	6.97 (n=5)

^a Potency and efficacy at human recombinant β_2 -adrenoceptors expressed in CHO cells assessed as elevations in cAMP. In this assay, all compounds appeared to be full agonists in comparison to isoprenaline control. ^b Ratio of EC₅₀ values generated at human recombinant β_1 - and β_2 -adrenoceptors expressed in CHO cells assessed as elevations in cAMP. Ratio is quoted to 2 significant figures. ^c EC₅₀ potency in the in vitro guinea pig trachea assay, quoted relative to salmeterol, such that a compound twice as potent will be quoted as 0.5. ^d Duration of action (DoA) was calculated as the time taken in hours for the EFS response to recover by 50% of the inhibition induced by an E_{\max} concentration of the test compound. ^e n.d.: EC₅₀ and potency relative to salmeterol not determined to facilitate rapid assessment of duration of action at an estimated E_{\max} concentration of test compound.

analogues were the most polar phenolic sulfonamides tested, again demonstrating the important relationship between lipophilicity and DoA in this template. In the case of **35** (log *D* = 1.1), it appears that the two methyl groups are insufficient lipophilic compensation for the addition of the polar phenol. However, dichlorophenol **34** is essentially isolipophilic with its regioisomer **33** but has a considerably lower log *D* (0.8 vs 2.0). The rational explanation for this effect relates to differences in ionization. Specifically, the two flanking chlorine atoms in **34** render the adjacent phenol much more acidic and prone to ionization, as reflected by a lower measured log *D*. This hypothetical level of acidity for **34** is supported by a measured p*K*_a value of 6.69, compared to chlorophenol **32** (9.22) and dimethylphenol **35** (9.93). This trend is consistent with widely understood electronic effects and clearly illustrates that this 2,6-dichlorophenol motif is approximately 3 orders of

magnitude more acidic than a standard phenol and only 2 orders of magnitude less acidic than acetic acid. Nevertheless, the majority of in vitro GPT data for **30**–**38** confirmed that this phenolic sulfonamide template could deliver the β_2 -adrenoceptor agonist pharmacology that we required, with obvious potential for crystallinity.²²

Compound **38** is essentially isolipophilic with salmeterol, so it is possible that lipophilicity drives its DoA, as proposed for both formoterol and salmeterol by the diffusion microkinetic hypothesis^{23,24} and as recently illustrated for indacaterol.³ However, the receptor exosite hypothesis has also been proposed to rationalize the long duration of action of salmeterol and recent analogues.^{1,18,25,26} High affinity binding of the long side chain deep into a hydrophobic core domain of the receptor effectively anchors the molecule and allows the saligenin headgroup to continuously activate the β_2 -adrenoceptor.

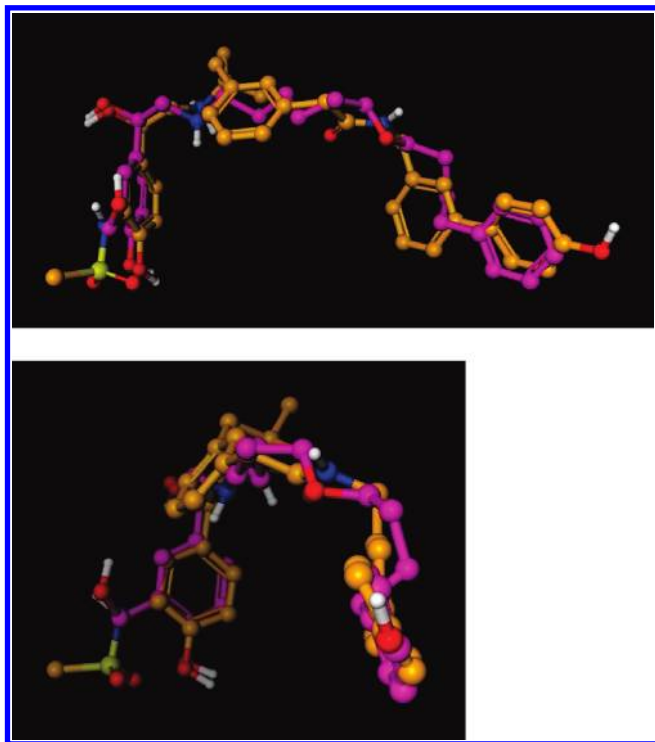


Figure 2. Structural overlays of **38** with salmeterol (purple).

Although there is significantly less conformational flexibility in the sulfonamide template compared to salmeterol, structural overlays suggest that salmeterol and **38** may be able to adopt similar conformations (Figure 2), as previously proposed for indole analogue **1**.⁷ It can be seen that when the key β_2 -adrenoceptor agonist headgroups are overlaid, the terminal aromatic tail residues occupy similar regions of space. Furthermore, the position of the amide moiety in **38** may serve to make receptor interactions similar to those made by the ether oxygen atom in the salmeterol tail. On the basis of these overlays, it can also be hypothesized that **38** retains the potential to access the proposed receptor exosite and that this drives its prolonged DoA.

In a manner consistent with initial sulfonamides such as **26** and **28**, the solid form of phenolic analogues **30–38** was highly encouraging, with many compounds isolated as solids directly from the final desilylation reaction by simple filtration. This ease of isolation enabled rapid PXRD analysis and early solid form assessment, identifying analogues such as **32**, **33**, **36**, **37**, and **38** with good levels of crystallinity. PXRD data were of such importance to us that these data were available for biaryl **38** prior to the emergence of biological data. Further solid form analysis of these compounds using well-known techniques such as DSC, TGA, and DVS identified **38** in particular as a compound with the most suitable combination of pharmacology and material properties. **38** possessed a highly crystalline, nonhygroscopic (1.7% water uptake at 90% relative humidity) solid form with high melting point (198 °C), material properties that were consistent with our solid form requirements.

With favorable material properties secured, the solid state compatibility of **38** was assessed with lactose monohydrate, the most common carrier excipient used in commercial dry power inhalers (DPI). Material blended at a 1:100 ratio with lactose monohydrate was shown to be stable after 8 weeks of storage at 40 °C and 75% relative humidity in open vials. These data for **38** demonstrated that crystalline β_2 -adreno-

Table 3. Pulmonary and Cardiovascular TI Data for **38**, **1**, Formoterol, and Salmeterol following Intratracheal Solution Administration to Anesthetized Dogs

compd	lung ED ₅₀ ^a (μg)	lung DoA at ED ₅₀ ^b (h)	lung DoA at 10 × ED ₅₀ ^b (h)	TI ^c lung vs CV
38	0.1	>8	>8	≥10
1	1	>8	>8	10
formoterol	0.1	4	<6	1
salmeterol	1	4	<7	1

^a ED₅₀ is the intratracheal dose giving 50% inhibition of ACh induced bronchoconstriction. ^b DoA was assessed by comparison of the airway resistance at 1 h intervals for a single dose of the test compound relative to the control ACh response. ^c TI (therapeutic index) is the inverse ratio of lung ED₅₀ compared to dose that caused the first increase in CV parameters.

receptor agonists from this sulfonamide template were suitable for inhaled dry-powder delivery, thus securing one aspect of our key project objectives.

With encouraging in vitro pharmacology and solid form data in hand, **38** was profiled in an anesthetized dog model of bronchoconstriction to assess in vivo efficacy, DoA, and cardiovascular (CV) side effects (e.g., heart rate).^{27,28} Anesthetized and artificially ventilated dogs were challenged with iv bolus doses of acetylcholine (ACh) to establish a dose that gave a transient 60–100% increase in lung resistance (R_L). A dose of either β_2 agonist or vehicle (micelle) was then delivered intratracheally (it.) before animals were rechallenged with ACh to compare R_L and CV parameters to the control ACh response. In this model, **38** was found to be equipotent to formoterol (ED₅₀ = 0.1 μg) and more potent than both salmeterol and development candidate **1** (ED₅₀ = 1 μg) (Table 3). At the ED₅₀ dose, **38** displayed similar intrinsic DoA to **1**, superior to both salmeterol and formoterol. Furthermore, a 10-fold higher dose of **38** (1 μg) afforded even greater efficacy and DoA, as illustrated against 1 μg of salmeterol (Figure 3). In addition, hemodynamic data from these studies confirmed that while salmeterol (1 μg) showed a trend toward increased heart rate, **38** did not induce tachycardia at the doses tested (Figure 3). These comparative data to b.i.d. clinical agents in a well validated in vivo model suggested encouraging potential for **38** to deliver 24 h duration of action in humans with a therapeutic index of at least 10-fold.

Compound **38** was subsequently profiled through a variety of in vitro pharmacokinetic (PK) assays (Table 4). Rapid CYP-mediated metabolism in a human microsomal assay (Cl_{int} = 54 (μL/min)/mg) and low to moderate cell permeability with high transporter mediated efflux ($P_{app}(A-B)$ < 1×10^{-6} cm/s, $P_{app}(B-A)$ = 13×10^{-6} cm/s) as measured by apical to basal flux rate through a monolayer of Caco-2 cells were observed. These in vitro data suggested that **38** would have low oral bioavailability due to poor absorption through the gut lumen and high first pass metabolism and warranted further progression of **38** to rat in vivo pharmacokinetic studies (Table 4).^{29,30} Following iv administration the volume of distribution was high (31 L/kg); however, with total clearance exceeding liver blood flow (103 (mL/min)/kg) the measured half-life was 3.5 h. Plasma protein binding in rat of 95% also gave very high unbound clearance (>2000 (mL/min)/kg). Following po administration in rat, the oral bioavailability was found to be <5%, consistent with predictions from in vitro data. Furthermore, analysis of rat portal vein samples confirmed that this was driven by fundamentally poor intestinal absorption with portal bioavailability of **38** also of <5%.

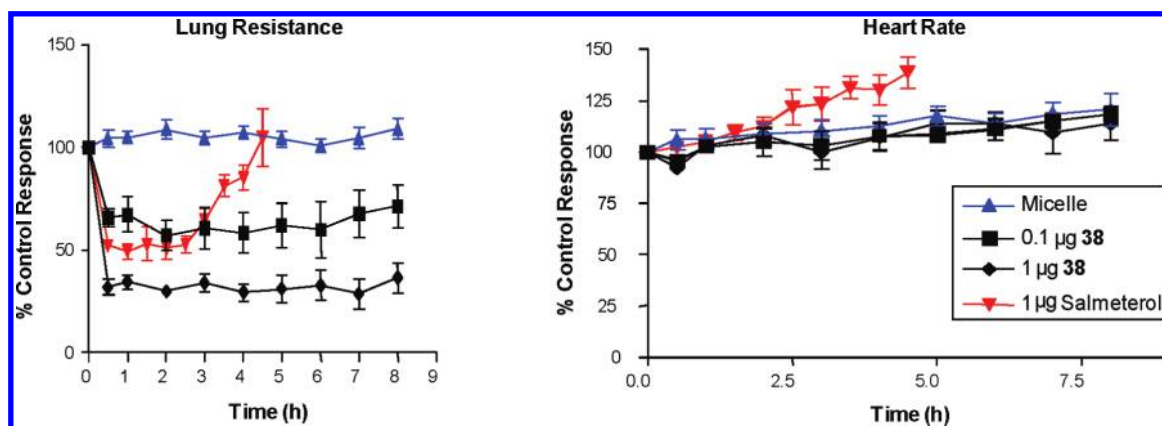


Figure 3. Respiratory and cardiovascular data for **38** and salmeterol following intratracheal administration to anesthetized dogs as solutions in micelle vehicle. Data are expressed as the percent change from pretreatment values, taking the pretreatment value as 100. Data are mean \pm SEM of $n = 4$ /group.

The metabolites of **38** were determined from numerous in vitro studies (human, rat, and dog hepatocytes and liver microsomes) and an in vivo isolated perfused rat liver (IPRL) study. The major metabolites observed were the glucuronide conjugate consistent with phase II conjugation on the hydroxy biphenyl moiety, the primary amide resulting from N-dealkylation of the biphenyl moiety, and the carboxylic acid resulting from amidolysis. The sulfate conjugate of **38** was also observed indicating additional phase II metabolism. Approximately 6% of the dose of **38** was excreted unchanged in the bile. By use of synthetic standards for analysis, none of these metabolites were found to circulate in any in vivo samples (IPRL perfusate or plasma). The extent of glucuronidation of **38** was further assessed in vitro using glucuronidation specific human liver microsome methodology and clinical standards similar to those described in the literature.³¹ Under these conditions **38** had a short half-life ($Cl_{int} = 33$ ($\mu\text{L}/\text{min}$)/mg) that suggested an unbound intrinsic clearance of > 10000 (mL/min)/kg. Glucuronidation was also observed in vitro for analogues **32** and **36**. Factoring in liver blood flow and human plasma protein binding, **38** was predicted to exhibit very high intrinsic clearance in humans due to glucuronidation. This successful introduction of phenolic glucuronidation as an additional route of metabolism to maximize clearance, TI and mitigate potential drug–drug interactions (DDI) was entirely consistent with our design strategy.

Additional studies in human liver microsomes with the addition of the cytochrome P450 3A4 inhibitor ketoconazole significantly reduced the intrinsic clearance of **38** ($Cl_{int} < 10$ ($\mu\text{L}/\text{min}$)/mg), suggesting that approximately 80% of phase I metabolism was mediated by CYP3A4. This observation was confirmed by experiments using expressed human CYP enzymes. In the absence of CYP3A4 metabolism the most significant CYP enzyme involved in the metabolism of **38** was found to be the polymorphically expressed enzyme CYP2D6.

Following intratracheal (it.) solution administration of **38** (100 μg) to rats, the rate of absorption from the lung into the

systemic compartment was found to be significantly slower than salmeterol, resulting in longer T_{max} (0.5 h vs 0.1 h) and lower systemic unbound C_{max} (1.3 nM vs 23 nM). These differences in absorption rate and exposure are illustrated by the it. PK profiles of both **38** and salmeterol (Figure 4). It is worth noting that the it. PK profile of salmeterol is identical to its iv PK profile, further illustrating its rapid absorption from the lung. In contrast, the it./iv PK profiles of **38** are markedly different, resulting in the observed 18-fold lower systemic unbound C_{max} relative to salmeterol.

Overall, **38** exhibited an ideal pharmacokinetic profile for an inhaled agent. In contrast to salmeterol, data following it. administration indicated potential for delayed but complete absorption from the lung in humans. Furthermore, the swallowed fraction of the dose was unlikely to contribute to systemic exposure or associated adverse events in humans due to incomplete oral absorption and extensive hepatic first pass extraction. In addition, high intrinsic clearance predicted in humans via multiple routes of metabolism suggested that unbound exposure of **38** arising from the lung absorbed dose should be minimal. Glucuronidation was predicted to be a major route of clearance of **38** in humans, leading to a low potential for drug–drug interactions. This pharmacokinetic profile suggested that, relative to salmeterol, compound **38** should demonstrate reduced systemically mediated adverse events arising from both the inhaled and swallowed fraction of the dose following inhalation in humans.³²

From a drug safety perspective, **38** showed no significant affinity (>100 nM) when evaluated for broader pharmacological activity against a wide ranging external panel of other receptors, enzymes, and ion channels. Furthermore, **38** had no meaningful functional effect on in vitro cardiac ion channel assays at micromolar concentrations (e.g., hERG patch clamp $IC_{50} > 10$ μM). In vitro genetic toxicity testing and in vivo rat toleration studies were also completed without observing any meaningful adverse effects. The tussivity of **38** was evaluated in a clinically validated rabbit lung cough model that measures action potentials from A δ -fibres/rapidly adapting receptors

Table 4. In Vitro and In Vivo Pharmacokinetic Data for Compound **38**

compd	in vitro PK			rat in vivo PK				
	HLM Cl_{int} (($\mu\text{L}/\text{min}$)/mg)	Caco-2 $P_{app} \times 10^{-6}$ (cm/s)		iv				po F (%)
		A–B	B–A	V_d (L/kg)	Cl_T ((mL/min)/kg)	$t_{1/2}$ (h)	rat ppb (%)	
38	54	<1	13	31	103	3.5	95	<5

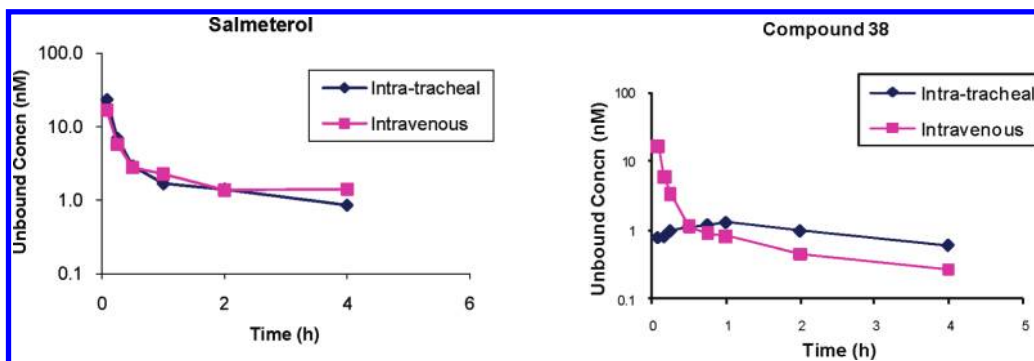
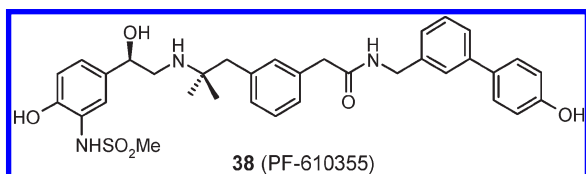


Figure 4. Pharmacokinetic profiles for salmeterol and **38** following intratracheal and intravenous administration of 100 μg solution formulations to rats.

Chart 5



(RAR).²⁷ This enables early assessment of the potential to cause cough, which is a key attrition risk for inhaled compound development. Indacaterol, an inhaled long acting β_2 -adrenoreceptor agonist that has been reported to cause postinhalational cough in humans, was also found to be tussive in this rabbit cough model.³³ In contrast, both **38** and salmeterol (nontussive in humans) were inactive in this model, thus providing confidence that **38** was unlikely to cause cough in humans. Overall, **38** had a preclinical safety profile that suggested it should be well tolerated in humans at all clinically relevant inhaled doses.

Conclusion

In conclusion, we have described our “inhalation by design” strategy to deliver a novel β_2 -adrenoreceptor agonist (**38**) that has longer duration of action in preclinical models than salmeterol, with clear potential for once-daily inhaled administration in humans via a dry-powder inhaler. Material properties were secured early through incorporation of the sulfonamide moiety in the headgroup as a key design feature to provide higher intrinsic crystallinity and to simplify solid form selection. Compound **38** exhibits an ideal preclinical pharmacokinetic profile for an inhaled agent by virtue of delayed lung absorption, negligible oral bioavailability, and high intrinsic clearance via multiple routes of metabolism, including extensive phenolic glucuronidation. Furthermore, the preclinical safety profile of **38** suggests that it will be well tolerated in humans at all clinically relevant doses. Given this exciting profile, **38** (PF-610355) was nominated as a development candidate (Chart 5), a novel once-daily inhaled β_2 -adrenoreceptor agonist for the treatment of asthma and COPD. Recent data (sGAW) from healthy volunteers in phase Ib clinical trials illustrate that **38** does indeed provide 24 h of bronchodilation from a single inhaled dose, thus confirming **38** as a once-daily inhaled β_2 -adrenoreceptor agonist (ultra-LABA) (Figure 5).³⁴ Compound **38** has achieved positive proof-of-concept (PoC) for the treatment of asthma and COPD and is currently in advanced phase II clinical studies.³⁵ Further information relating to **38** will be reported in future disclosures.

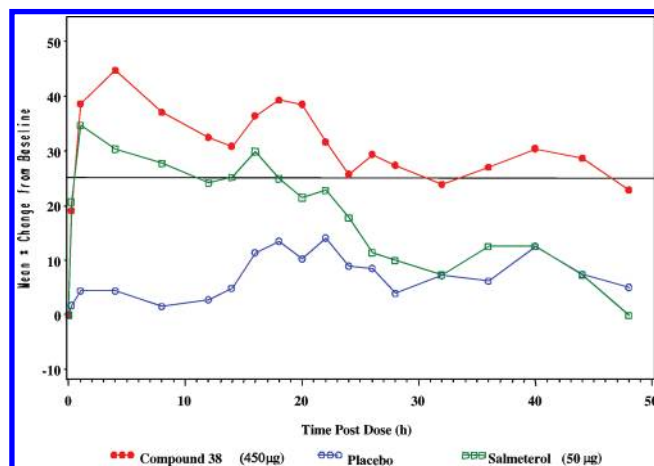


Figure 5. Phase Ib data from healthy human volunteers for **38** and salmeterol following inhalation of dry-powder formulations. Data are expressed as the mean percent change in sGAW from baseline by treatment.

Experimental Section

Biology. In Vitro Potency and Selectivity at Recombinant Human β_1 - and β_2 -Adrenoreceptors Expressed in CHO Cells. Chinese hamster ovary (CHO) cells separately expressing recombinant human β_1 - and β_2 -adrenoreceptors were generated using conventional cloning and PCR techniques. Cells were suspended in Flashplate stimulation buffer containing 0.5 mM IBMX (isobutylmethylxanthine), and 50 μL /well was added to the Flashplate containing the test compound. Each plate also contained control wells of isoprenaline (100 nM to measure maximum cAMP production) and 1% DMSO (to measure basal cAMP production). Plates were incubated at room temperature for 1 h. The cells were then lysed by addition of 100 μL /well Flashplate detection buffer containing ^{125}I -cAMP at 0.18 $\mu\text{Ci}/\text{mL}$ and the plates incubated at room temperature for a further 2 h prior to measurement of cAMP produced in the assay. Data were expressed as a percentage of the cAMP generated with isoprenaline and plotted against the concentration of agonist on a log scale. A four-parameter sigmoid fit was used to generate EC_{50} and E_{max} (%).

In Vitro Potency and Duration of Action in Guinea Pig Isolated Trachea. Tracheas were removed from male Dunkin–Hartley guinea pigs (475–525 g), cut into strips, and mounted in 5 mL organ baths in warmed (37 $^{\circ}\text{C}$) and aerated (95% O_2 /5% CO_2) Krebs solution (flow rate 1 mL/min) containing indomethacin (3 mM) and guanethidine (10 mM) under 1 g weight initial tension. Tissues were retensioned to 1 g every 15 min for 1 h and then subjected to electrical field stimulation (EFS: 0.1 ms, 10 Hz for 10 s every 2 min) at submaximal voltage (10–30 V). A single bolus concentration of test compound was added to each tissue

and left for 4 h. A concentration–response curve to test compound was constructed across tissues, and data were expressed as percent inhibition of the control contraction size. Following the 4 h incubation, tissues were washed initially at 90 mL/min for 1 min and then for 1 mL/min for the remainder of the experiment (up to 16 h). Duration of action (DoA) was calculated as the time taken in hours for the EFS response to recover by 50% of the inhibition induced by the test compound.

In Vivo Potency and Duration of Action in the Anesthetized Dog. Female beagle dogs (10–15 kg) were anesthetized with chloralose/urethane (100 (mg/mL)/kg, iv infusion) and maintained throughout the experiment with continuous iv infusion (1 (mL/kg)/h). The trachea was cannulated and connected to a large animal constant volume respirator (Ugo Basile 5025). Respiratory parameters (transpulmonary pressure (PTP) and flow) were monitored using differential pressure transducers. Blood pressure and left ventricular pressure were also monitored. Signals were analyzed using Ponemah software package PCR to determine lung resistance. Challenges of iv acetylcholine (ACh) were administered in the right femoral vein. Cardiovascular (CV) and respiratory parameters were measured before and after exposure to iv ACh (10 min intervals) to establish a dose that gave a change in lung resistance of between 60% and 100% over basal.

(i) For the dose response study, up to five doses of test compound or vehicle were given via intratracheal administration at cumulative 1 h intervals. The established iv dose of ACh was repeated 1 h after test compound administration to compare airway resistance and CV parameters to the control ACh response.

(ii) For the duration of action study, one dose of test compound or vehicle was administered intratracheally and ACh challenge (iv) repeated at 1 h intervals for up to 8 h to compare airway resistance and CV parameters to the control ACh response.

Chemistry. Unless otherwise indicated, all reactions were carried out under a nitrogen atmosphere, using commercially available anhydrous solvents. “0.880 Ammonia” refers to commercially available aqueous ammonia solution of 0.880 specific gravity. Thin-layer chromatography was performed on glass-backed precoated Merck silica gel (60 F254) plates, and compounds were visualized using UV light, 5% aqueous potassium permanganate, or chloroplatinic acid/potassium iodide solution. Silica gel column chromatography was carried out using 40–63 μ m silica gel (Merck silica gel 60). Ion exchange chromatography was performed using Isolute strong cation exchange resin (SCX-2) cartridges which had been prewashed with methanol. Proton NMR spectra were measured on a Varian Inova 400 or Varian Mercury 400 spectrometer in the solvents specified. In these NMR spectra, exchangeable protons that appeared distinct from solvent peaks are also reported. Low resolution mass spectra were recorded on either a Fisons Trio 1000, using thermospray positive ionization, or a Finnigan Navigator, using electrospray positive or negative ionization. High resolution mass spectra were recorded on a Bruker Apex II FT-MS using electrospray positive ionization. Test compound purity of $\geq 95\%$ was determined using combustion analysis conducted by Exeter Analytical U.K. Ltd., Uxbridge, Middlesex, U.K. Optical rotations were determined at 25 °C using a Perkin-Elmer 341 polarimeter using the solvents and concentrations specified.

N-{2-(Benzyloxy)-5-[(1*R*)-2-bromo-1-hydroxyethyl]phenyl}-methanesulfonamide (5). A solution of (1*R*)-1-[3-amino-4-(benzyloxy)phenyl]-2-bromoethanol **4**¹¹ (30.8 g, 95.6 mmol) in dichloromethane (300 mL) was treated with pyridine (9.30 mL, 115 mmol). The resulting solution was cooled to 5 °C and a solution of methanesulfonyl chloride (7.80 mL, 101 mmol) in dichloromethane (10 mL) added dropwise. The mixture was stirred at 5 °C for a further 30 min and then allowed to warm to room temperature over 16 h. The reaction mixture was washed with 2 M hydrochloric acid (110 mL), the organic phase separated, dried (magnesium sulfate), and the

solvent removed in vacuo to give an orange oil. The residue was crystallized from hot toluene (100 mL) to give **5** as a pale pink solid, 33.7 g, 88% yield. ¹H NMR (DMSO-*d*₆, 400 MHz) δ : 2.93 (s, 3H), 3.52–3.66 (m, 2H), 4.74 (m, 1H), 5.19 (s, 2H), 7.11 (d, 1H), 7.19–7.22 (m, 1H), 7.33–7.36 (m, 2H), 7.40–7.43 (m, 2H), 7.56 (d, 2H), 8.95 (s, 1H) ppm. LRMS: *m/z* 398–400 [M – H][–].

N-[2-(Benzyloxy)-5-[(1*R*)-2-bromo-1-[(*tert*-butyl(dimethyl)silyl]oxy)ethyl]phenyl]methanesulfonamide (6). Bromide **5** (21.5 g, 53.7 mmol) in *N,N*-dimethylformamide (125 mL) was treated with imidazole (4.16 g, 75.2 mmol) and *tert*-butyl(dimethyl)silylchloride (9.73 g, 64.5 mmol), and the resulting solution was stirred at room temperature for 16 h. The reaction mixture was diluted with ethyl acetate (200 mL) and washed with water (2 \times 100 mL). The aqueous phases were combined and extracted with ethyl acetate (100 mL). The combined organic extracts were washed with 2 M hydrochloric acid (100 mL), dried (magnesium sulfate), and concentrated in vacuo. The residue was triturated twice from pentane/ethyl acetate (200 mL, 1:1 by volume) and dried in vacuo to give **6** as a colorless solid, 23.7 g, 86% yield. ¹H NMR (CDCl₃, 400 MHz) δ : –0.07 (s, 3H), 0.11 (s, 3H), 0.89 (s, 9H), 2.91 (s, 3H), 3.40–3.50 (m, 2H), 4.80–4.83 (m, 1H), 5.14 (s, 2H), 6.80 (bs, 1H), 6.98 (d, 1H), 7.12 (d, 1H), 7.36–7.44 (m, 5H), 7.52–7.54 (m, 1H) ppm.

Diethyl 2,2'-(1,3-Phenylene)diacetate (11). 2,2'-(1,3-Phenylene)diacetic acid (10.0 g, 51.0 mmol) was dissolved in ethanol (100 mL) and the solution treated dropwise with catalytic acetyl chloride (2.50 mL). The reaction mixture was stirred at reflux for 18 h and then cooled to room temperature and concentrated in vacuo. The residue was taken up in ethyl acetate (100 mL) and extracted with sodium bicarbonate solution (3 \times 50 mL) and brine (3 \times 50 mL). The organic phase was then dried (magnesium sulfate) and concentrated in vacuo. The residue was triturated with pentane to give **11**, 11.8 g, 92% yield. ¹H NMR (CDCl₃, 400 MHz) δ : 1.31 (t, 6H), 3.65 (s, 4H), 4.20 (q, 4H), 7.24–7.36 (m, 4H) ppm. LRMS: *m/z* 251 [M + H]⁺.

[3-(2-Ethoxy-2-oxoethyl)phenyl]acetic Acid (12). A solution of the diester **11** (44.3 g, 177 mmol) and 2,2'-(1,3-phenylene)diacetic acid (59.2 g, 308 mmol) in ethanol (24 mL) and dioxane (290 mL) was treated dropwise with 12 M hydrochloric acid (4.90 mL, 58.8 mmol). The reaction mixture was stirred at reflux for 18 h, then cooled to room temperature and concentrated to low volume. The reaction mixture was diluted with toluene (125 mL) and the resulting slurry filtered. The filtrate was concentrated in vacuo and the residue taken up in water and basified with sodium bicarbonate until neutral pH was obtained. The mixture was diluted with ethyl acetate (200 mL), and the organic layer was separated and washed with sodium bicarbonate solution (5 \times 30 mL) and brine (50 mL). The combined aqueous extracts were acidified to pH 3 with 6 M hydrochloric acid and extracted with ether (3 \times 30 mL). The organic layers were combined, dried (magnesium sulfate), and concentrated in vacuo. The residue was triturated with pentane to give **12** as a colorless solid, 10.8 g, 27% yield. ¹H NMR (CD₃OD, 400 MHz) δ : 1.25 (t, 3H), 3.60 (m, 2H), 3.63 (m, 2H), 4.15 (q, 2H), 7.18–7.32 (m, 4H) ppm. LRMS: *m/z* 245 [M + Na]⁺.

[3-(2-Hydroxy-2-methylpropyl)phenyl]acetic Acid (13). Methylmagnesium chloride (51.0 mL of a 3 M solution in tetrahydrofuran, 153 mmol) was added dropwise to a stirred solution of **12** (11.6 g, 51.0 mmol) in tetrahydrofuran (300 mL) at 0 °C under nitrogen. The mixture was allowed to warm to room temperature overnight with the formation of a thick white precipitate. Water (50 mL) and 2 M hydrochloric acid (80 mL) were cautiously added. The aqueous layer was extracted with ethyl acetate (2 \times 300 mL), the combined organic layers were washed with brine (50 mL) and dried (sodium sulfate), and the solvent was removed in vacuo to give **13** as a golden oil, 11.2 g, 100% yield. ¹H NMR (CDCl₃, 400 MHz) δ : 1.22 (6H, s), 2.75 (2H, s), 3.63 (2H, s), 7.12–7.30 (4H, m) ppm. LRMS: *m/z* 209 [M + H]⁺.

(3-{2-[(Chloroacetyl)amino]-2-methylpropyl}phenyl)acetic Acid (14). 2-Chloroacetonitrile (8.80 mL, 140 mmol) was added to a solution of alcohol **13** (16.0 g, 70.0 mmol) in acetic acid (33 mL).

The resulting solution was cooled to 0 °C, treated with concentrated sulfuric acid (33 mL) and the reaction mixture allowed to warm to room temperature. After 4 h the reaction mixture was poured onto ice and basified with solid sodium carbonate. The solution was extracted with ethyl acetate (2 × 500 mL) and the combined organic extracts were dried (magnesium sulfate) and concentrated in vacuo to give **14** as a colorless solid, 19.0 g, 96% yield. ¹H NMR (CDCl₃, 400 MHz) δ: 1.36 (s, 6H), 3.02 (s, 2H), 3.62 (s, 2H), 3.95 (s, 2H), 6.19 (m, 1H), 7.06–7.31 (m, 4H) ppm. LRMS: *m/z* 282 [M – H][–].

[3-(2-Amino-2-methylpropyl)phenyl]acetic Acid Methyl Ester (10). A solution of amide **14** (5.10 g, 18.0 mmol), thiourea (1.60 g, 21.0 mmol), and acetic acid (18 mL) in ethanol (80 mL) was heated to reflux under a nitrogen atmosphere for 16 h. The reaction mixture was allowed to cool to room temperature and filtered. The filtrate was concentrated in vacuo, the residue dissolved in methanol (150 mL), saturated with hydrogen chloride gas, and the resulting solution heated to reflux for 16 h. The mixture was concentrated in vacuo and the residue partitioned between ethyl acetate (200 mL) and 5% aqueous sodium carbonate solution (200 mL). The organic phase was washed with brine (100 mL), dried (magnesium sulfate), and concentrated in vacuo. The residue was purified by strong cation exchange resin, eluting with methanol followed by a 2 M solution of ammonia in methanol, to give **10** as a yellow oil, 2.68 g, 67% yield. ¹H NMR (CDCl₃, 400 MHz) δ: 1.14 (s, 6H), 2.68 (s, 2H), 3.62 (s, 2H), 3.69 (s, 3H), 7.08–7.16 (m, 3H), 7.23–7.27 (m, 1H) ppm. LRMS: *m/z* 222 [M + H]⁺.

(3-{2-[(2R)-2-(4-Benzyloxy-3-methanesulfonylamino)phenyl]-2-(tert-butylidimethylsilyloxy)ethylamino]-2-methylpropyl}-phenyl)acetic Acid Methyl Ester (16). Amine **10** (36.0 g, 153 mmol) and bromide **6** (36.0 g, 70.8 mmol) were heated together at 85 °C for 72 h. The reaction mixture was cooled to room temperature and purified by column chromatography on silica gel, eluting with pentane/ethyl acetate (50:50, by volume) to give **16** as a pale yellow oil, 37.2 g, 80% yield. ¹H NMR (CDCl₃, 400 MHz) δ: –0.15 (s, 3H), 0.00 (s, 3H), 0.83 (s, 9H), 1.01 (s, 3H), 1.04 (s, 3H), 2.57–2.97 (m, 7H), 3.59 (s, 2H), 3.68 (s, 3H), 4.68–4.72 (m, 1H), 5.09 (s, 2H), 6.79 (bs, 1H), 6.95 (d, 1H), 7.04–7.21 (m, 7H), 7.37–7.44 (m, 5H), 7.56 (d, 1H) ppm. LRMS: *m/z* 655 [M + H]⁺.

Methyl (3-{2-[(2R)-2-(tert-Butylidimethylsilyloxy)-2-(4-hydroxy-3-(methylsulfonyl)amino)phenyl]ethylamino]-2-methylpropyl}phenyl)acetate (18). A solution of **16** (36.8 g, 56.0 mmol) in ethanol (550 mL) was treated with ammonium formate (16.0 g, 254 mmol) and 20% palladium hydroxide on carbon (1.50 g). The resulting suspension was heated to 85 °C for 2 h. Further 20% palladium hydroxide on carbon (1.00 g) was added, and heating continued for 1 h. The reaction mixture was cooled to room temperature, filtered and the solvent removed in vacuo. The residue was partitioned between ethyl acetate (500 mL) and 2 M aqueous ammonia (100 mL). The organic phase was separated, dried (magnesium sulfate) and the solvent removed in vacuo. The residue was purified by column chromatography on silica gel, eluting with dichloromethane/methanol/0.88 specific gravity ammonia (95:5:0.5, by volume) to give **18** as a pale yellow oil, 20.6 g, 65% yield. ¹H NMR (400 MHz, CDCl₃) δ: –0.17 (s, 3H), –0.05 (s, 3H), 0.80 (s, 9H), 1.07 (s, 3H), 1.09 (s, 3H), 2.66–2.91 (m, 7H), 3.62 (d, 2H), 3.69 (s, 3H), 4.71–4.74 (m, 1H), 6.58 (d, 1H), 6.88 (dd, 1H), 7.05–7.14 (m, 3H), 7.21–7.25 (m, 1H), 7.30 (s, 1H) ppm. LRMS: *m/z* 565 [M + H]⁺.

(3-{2-[(2R)-2-(tert-Butylidimethylsilyloxy)-2-(4-hydroxy-3-methanesulfonylamino)phenyl]ethylamino]-2-methylpropyl}phenyl)-acetic Acid (20). Ester **18** (20.6 g, 36.0 mmol) was dissolved in tetrahydrofuran (150 mL) and the solution treated dropwise with 1 M aqueous lithium hydroxide (72.0 mL, 72.0 mmol). The reaction mixture was stirred at room temperature for 72 h. The reaction mixture was neutralized by addition of 1 M hydrochloric acid (72.0 mL, 72.0 mmol) and concentrated in vacuo to low volume. The aqueous phase was decanted and the residue washed with water (2 × 50 mL). The residue was redissolved in tetra-

hydrofuran (50 mL) and toluene (50 mL) and the solvent removed in vacuo to give **20** as a pale brown foam, 20.2 g, 100% yield. ¹H NMR (400 MHz, CD₃OD) δ: –0.14 (s, 3H), 0.07 (s, 3H), 0.83 (s, 9H), 1.32 (m, 6H), 2.93 (m, 5H), 3.23 (m, 2H), 3.54 (m, 2H), 4.94 (m, 1H), 6.91 (d, 1H), 7.03–7.16 (m, 3H), 7.26 (m, 2H), 7.60 (m, 1H) ppm.

2-[3-(2-{[(2R)-2-(tert-Butyl(dimethyl)silyloxy]-2-(4-hydroxy-3-[(methylsulfonyl)amino]phenyl)ethyl]amino}-2-methylpropyl)-phenyl)-N-[(4'-hydroxybiphenyl-3-yl)methyl]acetamide (38a). A solution of carboxylic acid **20** (2.80 g, 5.08 mmol) in *N,N*-dimethylformamide (60 mL) was treated with 1-hydroxybenzotriazole hydrate (0.755 g, 5.59 mmol), 3'-(aminomethyl)biphenyl-4-ol hydrochloride¹⁴ (1.20 g, 5.08 mmol), 1-(3-dimethylaminopropyl)-3-ethylcarbodiimide hydrochloride (1.07 g, 5.59 mmol), and triethylamine (1.49 mL, 10.7 mmol). The resulting suspension was stirred at room temperature for 18 h. The solvent was removed in vacuo and the residue partitioned between dichloromethane (100 mL) and saturated aqueous sodium bicarbonate solution (50 mL). The organic phase was separated and the aqueous phase extracted with dichloromethane/methanol (95:5 by volume, 2 × 20 mL). The combined organic extracts were washed with saturated aqueous sodium chloride (100 mL), dried (sodium sulfate), and the solvent was removed in vacuo. The residue was purified by column chromatography on silica gel, eluting with dichloromethane/methanol/0.88 specific gravity ammonia (95:5:0.5, by volume) to give **38a** as a white foam, 2.10 g, 56% yield. ¹H NMR (400 MHz, CD₃OD) δ: –0.19 (s, 3H), –0.02 (s, 3H), 0.79 (s, 9H), 0.99 (s, 3H), 1.02 (s, 3H), 2.56–2.66 (m, 3H), 2.80–2.83 (m, 1H), 2.85 (s, 3H), 3.53 (s, 2H), 4.40 (s, 2H), 4.65–4.68 (dd, 1H), 6.80–6.82 (d, 2H), 6.83–6.85 (d, 1H), 7.00–7.02 (d, 2H), 7.09 (s, 1H), 7.12–7.14 (d, 1H), 7.18–7.20 (m, 2H), 7.27–7.31 (dd, 1H), 7.33–7.40 (m, 5H) ppm. LRMS: *m/z* 730 [M – H][–], 732 [M + H]⁺, 754 [M + Na]⁺.

N-[(4'-Hydroxybiphenyl-3-yl)methyl]-2-[3-(2-{[(2R)-2-hydroxy-2-(4-hydroxy-3-[(methylsulfonyl)amino]phenyl)ethyl]amino}-2-methylpropyl)phenyl]acetamide (38, PF-610355). Compound **38a** (2.10 g, 2.87 mmol) was dissolved in ethanol (79.0 mL) and treated with a solution of ammonium fluoride (1.06 g, 28.7 mmol) in water (53.0 mL). The reaction mixture was stirred at 40 °C for 18 h, then cooled to room temperature. The reaction mixture was filtered and washed with methanol/water (1:1 by volume, 3 × 10 mL) and dried in vacuo to give **38** as a crystalline white solid, 1.55 g, 87% yield. ¹H NMR (400 MHz, DMSO-*d*₆) δ: 0.88 (s, 3H), 0.90 (s, 3H), 2.54–2.66 (m, 4H), 2.88 (s, 3H), 3.43 (s, 2H), 4.29–4.30 (d, 2H), 4.39–4.43 (dd, 1H), 6.79–6.82 (m, 3H), 6.96–7.01 (dd, 2H), 7.07–7.17 (m, 5H), 7.27–7.31 (dd, 1H), 7.36–7.41 (m, 4H), 8.50–8.53 (dd, 1H) ppm. HRMS: *m/z* 618.2607 [M + H]⁺, calcd 618.263782. [α]_D²⁰ –14.8° (c 0.392, methanol). Anal. (C₃₄H₃₉N₃O₆·0.3H₂O) C, H, N. HPLC analysis: ≥99.3% purity.

Acknowledgment. We thank Michele Coghlan, Christel Jones, Sheena Patel, and Susan Summerhill for their contributions to in vitro biology studies and John Adcock, Petra Chaffe, Tim Davies, Louise Sladen, and Karen Wright for in vivo biology studies. We also thank Ken Butcher, Sara Chunn, Tim Hobson, Louise Marples, Michael Paradowski, Dannielle Roberts, Keith Reeves, and Michelle Wilkes for assistance with the chemistry programme. Yogesh Sabnis is thanked for performing computational superpositions, Cheryl Doherty is thanked for her contributions to the X-ray structural information, and Fiona MacIntyre is also thanked for the provision of clinical data.

Supporting Information Available: Biology experimental details for the in vivo rabbit lung Aδ-fiber cough model; chemistry experimental details and analytical data for intermediates **8**, **9a**, **7**, **15**, **17**, **19**, **21a**–**37a** and test compounds **21**–**37**; X-ray data collection, structure solution, and ORTEP

plot for compound **26**; and general procedure for computational superposition of **38** and salmeterol. This material is available free of charge via the Internet at <http://pubs.acs.org>.

References

- Procopiou, P. A.; Barrett, V. J.; Bevan, N. J.; Biggadike, K.; Butchers, P. R.; Coe, D. M.; Conroy, R.; Edney, D. D.; Field, R. N.; Ford, A. J.; Guntrip, S. B.; Looker, B. E.; McLay, I. M.; Monteith, M. J.; Morrison, V. S.; Mutch, P. J.; Richards, S. A.; Sasse, R.; Smith, C. E. Synthesis and structure–activity relationships of long-acting β_2 adrenergic receptor agonists incorporating arylsulfonamide groups. *J. Med. Chem.* **2009**, *52*, 2280–2288.
- Beattie, D.; Bradley, M.; Brearley, A.; Charlton, S. J.; Cuenoud, B. M.; Fairhurst, R. A.; Gedec, P.; Gosling, M.; Janus, D.; Jones, D.; Lewis, C.; McCarthy, C.; Oakman, H.; Stringer, R.; Taylor, R. J.; Tuffnell, A. A physical properties based approach for the exploration of a 4-hydroxybenzothiazolone series of β_2 -adrenoceptor agonists as inhaled long-acting bronchodilators. *Bioorg. Med. Chem. Lett.* **2010**, *20*, 5302–5307.
- Baur, F.; Beattie, D.; Beer, D.; Bentley, D.; Bradley, M.; Bruce, I.; Charlton, S. J.; Cuenoud, B.; Ernst, R.; Fairhurst, R. A.; Fallor, B.; Farr, D.; Keller, T.; Fozard, J. R.; Fullerton, J.; Garman, S.; Hatto, J.; Hayden, C.; He, H.; Howes, C.; Janus, D.; Jiang, Z.; Lewis, C.; Loeuillet-Ritzler, F.; Moser, H.; Reilly, J.; Steward, A.; Sykes, D.; Tedaldi, L.; Trifileff, A.; Tweed, M.; Watson, S.; Wissler, E.; Wyss, D. The identification of indacaterol as an ultralong-acting inhaled β_2 -adrenoceptor agonist. *J. Med. Chem.* **2010**, *53*, 3675–3684.
- Cazzola, M.; Segreti, A.; Matera, M. G. Novel bronchodilators in asthma. *Curr. Opin. Pulm. Med.* **2010**, *16*, 6–12.
- Procopiou, P. A.; Barrett, V. J.; Bevan, N. J.; Biggadike, K.; Box, P. C.; Butchers, P. R.; Coe, D. M.; Conroy, R.; Emmons, A.; Ford, A. J.; Holmes, D. S.; Horsley, H.; Kerr, F.; Li-Kwai-Cheung, A.-M.; Looker, B. E.; Mann, I. S.; McLay, I. M.; Morrison, V. S.; Mutch, P. J.; Smith, C. E.; Tomlin, P. Synthesis and structure–activity relationships of long-acting β_2 adrenergic receptor agonists incorporating metabolic inactivation: an antedrug approach. *J. Med. Chem.* **2010**, *53*, 4522–4530.
- Bouyssou, T.; Hoenke, C.; Rudolf, K.; Lustenberger, P.; Pestel, S.; Sieger, P.; Lotz, R.; Heine, C.; Buettner, F. H.; Schnapp, A.; Konetzki, I. Discovery of olodaterol, a novel inhaled β_2 -adrenoceptor agonist with a 24h bronchodilatory efficacy. *Bioorg. Med. Chem. Lett.* **2010**, *20*, 1410–1414.
- Brown, A. D.; Bunnage, M. E.; Glossop, P. A.; Holbrook, M.; Jones, R. D.; Lane, C. A. L.; Lewthwaite, R. A.; Mantell, S.; Perros-Huguet, C.; Price, D. A.; Webster, R. The discovery of indole-derived long acting β_2 -adrenoceptor agonists for the treatment of asthma and COPD. *Bioorg. Med. Chem. Lett.* **2007**, *17*, 6188–6191.
- Brown, A. D.; Bunnage, M. E.; Glossop, P. A.; James, K.; Jones, R. D.; Lane, C. A. L.; Lewthwaite, R. A.; Mantell, S.; Perros-Huguet, C.; Price, D. A.; Trevethick, M.; Webster, R. The discovery of long acting β_2 -adrenoceptor agonists. *Bioorg. Med. Chem. Lett.* **2007**, *17*, 4012–4015.
- Brown, A. D.; Bunnage, M. E.; Glossop, P. A.; James, K.; Jones, R. D.; Lane, C. A. L.; Lewthwaite, R. A.; Mantell, S.; Perros-Huguet, C.; Price, D. A.; Trevethick, M.; Webster, R. The discovery of adamantyl-derived, inhaled, long acting β_2 -adrenoceptor agonists. *Bioorg. Med. Chem. Lett.* **2008**, *18*, 1280–1283.
- Glossop, P. A. Discovery and Selection of Inhaled Long-Acting β_2 -Adrenoceptor Agonists for Asthma and COPD. Presented at the ACS ProSpectives Conference: Discovery and Selection of Successful Drug Candidates, San Francisco, CA, May 4–7, 2008.
- Hett, R.; Fang, Q. K.; Gao, Y.; Wald, S. A.; Senanayake, C. H. Large-scale synthesis of enantio- and diastereomerically pure (*R*, *R*)-formoterol. *Org. Process Res. Dev.* **1998**, *2*, 96–99.
- Ritter, J. J.; Kalish, J. New reaction of nitriles. II. Synthesis of *t*-carbinamines. *J. Am. Chem. Soc.* **1948**, *70*, 4048–4050.
- Jirgensons, A.; Kauss, V.; Kalvinsh, I.; Gold, M. R. A practical synthesis of *tert*-alkylamines via the ritter reaction with chloroacetonitrile. *Synthesis* **2000**, *12*, 1709–1712.
- Brown, A. D.; Bunnage, M. E.; Glossop, P. A.; James, K.; Lane, C. A. L.; Lewthwaite, R. A.; Moses, I. B.; Price, D. A.; Thomson, N. M. A Preparation of Sulfonamide Derivatives of (Aminoethyl)-phenols, Useful for the Treatment of Allergic and Respiratory Diseases. U.S. Pat. Appl. Publ. US 2005182091, 2005.
- Veber, D. F.; Johnson, S. R.; Cheng, H.-Y.; Smith, B. R.; Ward, K. W.; Kopple, K. D. Molecular properties that influence the oral bioavailability of drug candidates. *J. Med. Chem.* **2002**, *45*, 2615–2623.
- Lipinski, C. A.; Lombardo, F.; Dominy, B. W.; Feeney, P. J. Experimental and computational approaches to estimate solubility and permeability in drug discovery and development settings. *Adv. Drug Delivery Rev.* **1997**, *23*, 3–25.
- Trofast, J.; Österberg, K.; Källström, B.-L.; Waldeck, B. Steric aspects of agonism and antagonism at β -adrenoreceptors: synthesis and pharmacological experiments with the enantiomers of formoterol and their diastereomers. *Chirality* **1991**, *3*, 443–450.
- Nials, A. T.; Sumner, M. J.; Johnson, M.; Coleman, R. A. Investigations into factors determining the duration of action of the β_2 -adrenoceptor agonist, salmeterol. *Br. J. Pharmacol.* **1993**, *108*, 507–515.
- Fisher, M. B.; Paine, M. F.; Strelevitz, T. J.; Wrighton, S. A. The role of hepatic and extrahepatic UDP-glucuronosyltransferases in human drug metabolism. *Drug Metab. Rev.* **2001**, *33*, 273–297.
- Freddolino, P. L.; Kalani, M. Y. S.; Vaidehi, N.; Floriano, W. B.; Hall, S. E.; Trabanino, R. J.; Kam, V. W. T.; Goddard, W. A., III. Predicted 3D structure for the human β_2 -adrenergic receptor and its binding site for agonists and antagonists. *Proc. Natl. Acad. Sci. U.S.A.* **2004**, *101*, 2736–2741.
- Manchee, G. R.; Barrow, A.; Kulkarni, S.; Palmer, E.; Oxford, J.; Colthup, P. V.; Maconopchie, J. G.; Tarbit, M. H. Disposition of salmeterol xinafoate in laboratory animals and humans. *Drug Metab. Dispos.* **1993**, *21*, 1022–1028.
- Coghlan, M.; Jones, C.; Summerhill, S.; Patel, S.; Clarke, N.; Trevethick, M.; Yeadon, M.; Perros-Huguet, C. The in vitro biology of PF-00610355: a novel β_2 -adrenoceptor agonist with a long duration of action. *Eur. Respir. J.* **2009**, *34* (S53), Abstract P2067.
- Anderson, G. P. Formoterol: pharmacology, molecular basis of agonism, and mechanism of long duration of a highly potent and selective β_2 -adrenoceptor agonist bronchodilator. *Life Sci.* **1993**, *52*, 2145–2160.
- Anderson, G. P.; Linden, A.; Rabe, K. F. Why are long-acting beta-adrenoceptor agonists long-acting? *Eur. Respir. J.* **1994**, *7*, 569–578.
- Johnson, M.; Butchers, P. R.; Coleman, R. A.; Nials, A. T.; Strong, P.; Summer, M. J.; Vardey, C. J.; Whelan, C. J. The pharmacology of salmeterol. *Life Sci.* **1993**, *52*, 2131–2143.
- Coleman, R. A.; Johnson, M.; Nials, A. T.; Vardey, C. J. Exosites: their current status, and their relevance to the duration of action of long-acting β_2 -adrenoceptor agonists. *TIPS* **1996**, *17*, 324–330.
- Sladen, L.; Wright, K.; Adcock, J.; Chaffe, P.; Clarke, N.; Yeadon, M.; Perros-Huguet, C. Effects of intra tracheal PF-00610355, an inhaled β_2 -adrenoceptor agonist, in anaesthetised animals. *Eur. Respir. J.* **2009**, *34* (S53), Abstract P2020.
- Wright, K.; Davies, T.; Clarke, N.; Yeadon, M.; Perros-Huguet, C. PF-00610355, an inhaled β_2 -adrenoceptor agonist with superior potency and duration of action (DoA) to salmeterol in the conscious dog model of bronchoconstriction. *Eur. Respir. J.* **2009**, *34* (S53), Abstract P2060.
- Artursson, P.; Palm, K.; Luthman, K. Caco-2 monolayers in experimental and theoretical predictions of drug transport. *Adv. Drug Delivery Rev.* **1996**, *22*, 67–84.
- Taburet, A. M.; Schmit, B. Pharmacokinetic optimization of asthma treatment. *Clin. Pharmacokinet.* **1994**, *26*, 396–418.
- Kilford, P. J.; Stringer, R.; Sohal, B.; Houston, J. B.; Galetin, A. Prediction of drug clearance by glucuronidation from in vitro data: use of combined cytochrome P450 and UDP-glucuronosyltransferase cofactors in alamethicin-activated human liver microsomes. *Drug Metab. Dispos.* **2009**, *37*, 82–89.
- Bennett, J. A.; Harrison, T. W.; Tattersfield, A. E. The contribution of the swallowed fraction of an inhaled dose of salmeterol to its systemic effects. *Eur. Respir. J.* **1999**, *13*, 445–448.
- Assessment Report for Onbrez Breezhaler; EMA/659981/2009; European Medicines Agency: London, Dec 17, 2009.
- MacIntyre, F.; Jones, I.; Surujbally, B. A randomised, double-blind study to determine the duration of action of lung pharmacodynamics by plethysmography (sGaw) of a β_2 -adrenoceptor agonist, PF-00610355. *Eur. Respir. J.* **2009**, *34* (S53), Abstract P2017.
- (a) Li, G. L.; MacIntyre, F.; Surujbally, B.; Chong, C. L.; Davis, J. Pharmacokinetics of PF-00610355, a novel inhaled long-acting β_2 -adrenoceptor agonist. *Eur. Respir. J.* **2009**, *34* (S53), Abstract E4354. (b) Li, G. L.; MacIntyre, F.; Surujbally, B.; Chong, C. L.; Davis, J. Safety and toleration of PF-00610355, a novel inhaled long acting β_2 -adrenoceptor agonist. *Eur. Respir. J.* **2009**, *34* (S53), Abstract P2018. (c) MacIntyre, F.; Jones, I.; Surujbally, B.; Scholl, D.; Bateman, E. A randomised double-blind, study to determine the efficacy and safety of a once-daily inhaled β_2 -adrenoceptor agonist, PF-00610355, in asthmatic patients. *Eur. Respir. J.* **2009**, *34* (S53), Abstract E4355. (d) Ribbing, J.; Li, G. L.; Van Schaick, E.; Harnisch, L. Assessing the therapeutic benefit of a new inhaled QD LABA through population PK-safety and efficacy modelling. *Eur. Respir. J.* **2009**, *34* (S53), Abstract P2021.